Toxicology in Vitro 29 (2015) 1172–1184

Contents lists available at ScienceDirect

Toxicology in Vitro

journal homepage: www.elsevier.com/locate/toxinvit

# Mechanism of neutrophil activation and toxicity elicited by engineered nanomaterials

Helinor Johnston [a,*], David M. Brown [a], Nilesh Kanase [a], Matthew Euston [b], Birgit K. Gaiser [a], Calum T. Robb [a,c], Elisabeth Dyrynda [a], Adriano G. Rossi [c], Euan R. Brown [b], Vicki Stone [a]

[a] School of Life Sciences, Heriot-Watt University, Edinburgh EH14 4AS, United Kingdom
[b] Institute of Biological Chemistry, Biophysics and Bioengineering, School of Engineering and Physical Sciences, Heriot-Watt University, Edinburgh EH14 4AS, United Kingdom
[c] MRC Centre for Inflammation Research, Queen's Medical Research Institute, University of Edinburgh, Edinburgh EH16 4TJ, United Kingdom

ARTICLE INFO

*Article history:*
Received 6 February 2015
Accepted 27 April 2015
Available online 8 May 2015

*Keywords:*
Nanomaterial
Neutrophil
Toxicity
Mechanism
$Ca^{2+}$

ABSTRACT

The effects of nanomaterials (NMs) on biological systems, especially their ability to stimulate inflammatory responses requires urgent investigation. We evaluated the response of the human differentiated HL60 neutrophil-like cell line to NMs. It was hypothesised that NM physico-chemical characteristics would influence cell responsiveness by altering intracellular $Ca^{2+}$ concentration $[Ca^{2+}]_i$ and reactive oxygen species production.

Cells were exposed (1.95–125 μg/ml, 24 h) to silver (Ag), zinc oxide (ZnO), titanium dioxide ($TiO_2$), multi-walled carbon nanotubes (MWCNTs) or ultrafine carbon black (ufCB) and cytotoxicity assessed (alamar blue assay). Relatively low ($TiO_2$, MWCNTs, ufCB) or high (Ag, ZnO) cytotoxicity NMs were identified. Sub-lethal impacts of NMs on cell function were investigated for selected NMs only, namely $TiO_2$, Ag and ufCB. Only Ag stimulated cell activation. Within minutes, Ag stimulated an increase in $[Ca^{2+}]_i$ (in Fura-2 loaded cells), and a prominent inward ion current (assessed by electrophysiology). Within 2–4 h, Ag increased superoxide anion release and stimulated cytokine production (MCP-1, IL-8) that was diminished by $Ca^{2+}$ inhibitors or trolox. Light microscopy demonstrated that cells had an activated phenotype.

In conclusion NM toxicity was ranked; Ag > ufCB > $TiO_2$, and the battery of tests used provided insight into the mechanism of action of NM toxicity to guide future testing strategies.



## 1. Introduction

Engineered nanomaterials (NMs) are defined as having at least one dimension that is 1–100 nm in size (European Commission, 2011). The properties of materials drastically change at the nanoscale, which has led to the incorporation of NMs in a variety of products and applications across different sectors (e.g. food, pharmaceutical, textiles, cosmetics). As the use of NMs increases worldwide their effects on biological systems, especially their ability to stimulate inflammatory responses, requires urgent investigation to better understand the risks to human health and the environment.

In the 1990s it was established that there was a link between exposure to particulate air pollution ($PM_{10}$) and adverse health effects in humans (e.g. Pope and Dockery, 1999). Subsequent studies then identified that the ultrafine component of $PM_{10}$ (equivalent to NMs, in terms of size) contributed to the adverse health effects observed (Peters et al., 1997; Seaton et al., 1995). Ultrafine particles had a detrimental impact on human health due to their ability to induce inflammation in the lung (e.g. Donaldson et al., 2001). The cellular and molecular mechanism by which these particles exhibit toxicity has been extensively investigated (e.g. Brown et al., 2000, 2001, 2004a; Ferin et al., 1992; Jiménez et al., 2002; Li et al., 2000, 2002; Möller et al., 2005; Oberdörster et al., 1992; Shukla et al., 2000; Stone et al., 1998, 2000; Wilson et al., 2002). A hypothesis was generated which suggested that the toxicity of ultrafine particles was related to their ability to stimulate reactive oxygen species (ROS) and $Ca^{2+}$ driven intracellular signaling cascades in pulmonary cells (e.g. macrophages, epithelial cells) which in turn activated transcription factors (e.g. nuclear factor kappa B (NF-κB)) to promote pro-inflammatory responses via changes in gene expression (Brown et al., 2004a; Donaldson et al., 2003; Li et al., 2003; Nel et al., 2006; Schmid et al., 2009; Stone et al., 2007; Xiao et al., 2003).

Despite the recent increase in the number of studies that assess the potential hazards posed by engineered NMs to human health there have been relatively few studies that have addressed the

* Corresponding author. Tel.: +44 (0) 131 451 3303; fax: +44 (0)131 451 3009.
*E-mail address:* h.johnston@hw.ac.uk (H. Johnston).

http://dx.doi.org/10.1016/j.tiv.2015.04.021
0887-2333/

mechanism of NM toxicity. However this information is required to enable the identification of novel, evidence based cellular responses to assess NM safety, as well as help to identify the consequences of NM exposure for human health. Indeed, this research need has been recently emphasised as a research priority in the area of nanotoxicology, as the information and data obtained will ultimately help deliver a more intelligent testing strategy to assess NM risk (Stone et al., 2014). Importantly, existing information on the mode of action of ultrafine particle toxicity can guide the experimental design of studies that investigate NM toxicity.

In this study, the mechanism underlying the cellular response to NMs was investigated in neutrophil-like differentiated HL60 cells. Neutrophils are phagocytic cells and a key component of the acute inflammatory response to foreign material (Goncalves et al., 2011). An infiltration of neutrophils into sites where NMs accumulate *in vivo* (rodents) is a common phenomenon following NM exposure, and has been observed at various target sites including the lungs (e.g. Baisch et al., 2014; Brown et al., 2001; Ferin et al., 1992; Jacobsen et al., 2009; Sayes et al., 2007), pleural cavity (e.g. Murphy et al., 2011), liver (e.g. Kermanizadeh et al., 2013a) and peritoneal cavity (e.g. Poland et al., 2008) for a variety of NM types (including ultrafine carbon black (ufCB), polystyrene, carbon nanotubes (CNTs), titanium dioxide ($TiO_2$), carbon fullerenes, gold, quantum dots, and silver (Ag)) and following administration via different routes (e.g. intratracheal instillation, inhalation, intravenous, intrapleural or intraperitoneal injection). Neutrophils also play a major role in the prolonged or chronic response to pathological particles (Brown et al., 1991; Donaldson et al., 1988). The increased expression and/or production of neutrophil chemoattractants (e.g. macrophage inflammatory protein 2 (MIP-2)) have been observed *in vivo* following exposure to NMs (e.g. Baisch et al., 2014; Gaiser et al., 2013). As such, neutrophil driven responses have been frequently used as a marker of the acute inflammatory response to NMs *in vivo* at different target sites. Furthermore, the release of neutrophil chemoattractants such as interleukin (IL)-8 or MIP-2 from macrophages (e.g. Park et al., 2011), epithelial cells (e.g. Baktur et al., 2011; Brown et al., 2001; Duffin et al., 2007; Monteiller et al., 2007), hepatocytes (e.g. Gaiser et al., 2013; Kermanizadeh et al., 2013b), renal epithelial cells (e.g. Kermanizadeh et al., 2013c), intestinal epithelial cells (e.g. Gerloff et al., 2013) and keratinocytes (e.g. Monteiro-Riviere et al., 2005; Samberg et al., 2010) has been observed *in vitro* following exposure to NMs (of various types). Thus understanding of the neutrophil response to NMs, and the consequences of this response for health is key to the risk assessment of NMs.

Despite extensive evidence of the prominent role of neutrophils in the response of various target sites in the body to NMs, there have been a limited number of studies that have investigated the consequences of neutrophil exposure to NMs. Several *in vitro* studies have demonstrated that NMs are able to stimulate neutrophil activation following exposure when the following parameters were investigated; respiratory/oxidative burst (Abrikossova et al., 2012; Couto et al., 2014), cytokine production (Gonçalves et al., 2010), neutrophil degranulation (Babin et al., 2013), changes in intracellular signaling (e.g. $Ca^{2+}$ flux (Brown et al., 2010)), cell death (Gonçalves et al., 2010), and etosis (Farrera et al., 2014; Haase et al., 2014; Jovanovic et al., 2011).

The aim of this study was to investigate the cell and molecular events underlying the response of neutrophil-like cells to NMs *in vitro*. In the first instance the cytotoxicity of a panel of NMs that varied with respect to their physico-chemical properties (including Ag, zinc oxide (ZnO), $TiO_2$, ultrafine carbon black (ufCB) and multi-walled carbon nanotubes (MWCNTs)) was screened in differentiated human HL60 cells. Investigation of the capacity of the NM panel to induce cytotoxicity was performed to identify sub-lethal concentrations of NMs to test in mechanistic studies. In addition, it allowed the toxicity of the NM panel to be ranked, and as a consequence the ability of selected NMs, namely Ag (a high toxicity NM) and $TiO_2$ (a relatively low toxicity NM) to impact on the activation status of cells was investigated in greater depth. Based on previous information regarding the toxicity of ultrafine particles we tested the hypothesis that the response of neutrophil-like cells to NMs will be driven by $Ca^{2+}$ and oxidant dependent signaling, and will vary according to NM physicochemical characteristics. ufCB was included in the study as previous studies have demonstrated that this particle type is able to activate neutrophils and macrophages via $Ca^{2+}$ and oxidant signaling (Brown et al., 2000, 2004a, 2004b, 2010). Endpoints investigated in this study were selected to enable assessment of neutrophil activation (e.g. cytokine production, respiratory burst, cell morphology) by NMs as well as the cell and molecular processes underlying these cell responses (e.g. intracellular $Ca^{2+}$ concentration, membrane ion current).

## 2. Materials and methods

All materials were purchased from Sigma–Aldrich (Poole, UK), unless otherwise stated.

### 2.1. NM panel, characterisation and preparation

$TiO_2$ (NM101), ZnO (NM110), MWCNT (NM400) and Ag (NM300) NMs were obtained from the nanomaterials repository at the Institute for Health and Consumer Protection at the European Commission Joint Research Centre in Ispra (Italy) (http://ihcp.jrc.ec.europa.eu/our_activities/nanotechnology/nanomaterials-repository). Ultrafine carbon black (ufCB, Printex 90) was obtained from Degussa (Frankfurt, Germany).

The NM panel being investigated in this study has been extensively characterised (Kermanizadeh et al., 2013a,b,c; Stone et al., 1998; Klein et al., 2011; Singh et al., 2011), and these data have been summarised in Table 1.

Ag NMs were supplied in de-ionised water (85%) with 7% stabilising agent (ammonium nitrate) and 8% emulsifiers (4% each of polyoxyethylene glycerol trioleate and Tween-20). All other materials were supplied as dry powders. Immediately prior to use, a 1 mg/ml stock of NMs in 2% fetal calf serum (FCS, in water) was prepared and sonicated for 16 min, following a protocol developed during the FP7 funded project ENPRA (Jacobsen et al., 2010). Following sonication, the NM suspensions were placed on ice. The NMs were then subject to serial dilutions in the appropriate medium for each assay of interest to the required concentration(s).

The hydrodynamic diameter of the NMs in biological media was investigated using Dynamic Light Scattering (DLS, Malvern Zeta Sizer Nano Series). Following sonication, the concentration of each NM was adjusted to 31 μg/ml in phenol red free complete cell culture medium (see below for details) and the NM hydrodynamic diameter and zeta potential measured. MWCNTs were not analysed as only spherical particles are suitable for DLS measurement.

### 2.2. HL60 cell culture and differentiation

The human HL60 suspension cell line has been widely used as a cell culture model of human neutrophils. HL60 cells were cultured in RPMI medium containing 2 mM L-glutamine, penicillin (100U) and streptomycin (100 μg/ml) and 10% FCS (termed complete cell culture medium). Cells were incubated at 37 °C, in an atmosphere of 5% $CO_2$. Prior to exposure to NMs, cells were differentiated into mature neutrophil-like cells using 1 μM all-*trans*-retinoic acid at a cell concentration of $0.2 \times 10^6$ cells/ml in 75 $cm^2$ plastic culture

**Table 1**
NM physico-chemical characteristics. Details of the NM, supplier and physico-chemical characteristics as provided by the supplier and those measured within existing studies are included. For more information on the physico-chemical characterisation of the NM panel please refer to Kermanidazeh et al. (2013b), Stone et al. (1998), Klein et al. (2011) and Singh et al. (2011). Briefly, transmission electron microscopy (TEM) was used to assess particle size and morphology, and surface area was measured using the Brunauer, Emmett and Teller (BET) method.

| NM | Supplier name | Supplier | Supplier information (diameter) | Size measurements (TEM) | Morphology (TEM) | Surface area ($m^2$/g) (BET) |
|---|---|---|---|---|---|---|
| $TiO_2$ (anatase) | NM 101 | JRC Repository | 7 nm | 4–8/50–100 nm | Agglomerates | 322 |
| Ag | NM 300 | JRC Repository | <20 nm | 8–47 nm | Mainly euhedral | NM supplied as a suspension: BET cannot be performed |
| MWCNT | NM 400 | JRC Repository | 30 nm diameter, 5 μm long | 5–35 nm diameter 700–3000 nm long | Entangled (10–20 walls) | 298 |
| ZnO | NM 110 | JRC Repository | 100 nm | 20–250 nm 50–350 nm | Euhedral | 14 |
| Ultrafine carbon black | Printex 90 | Degussa | 14 nm | 7–28.2 nm | Spherical | 254 |

flasks (30 ml total volume) for two days, as described previously (Brown et al., 2010).

### 2.3. Cytotoxicity assessment: alamar blue assay

Following differentiation, cells were seeded into the wells of a 96 well plate at a concentration of $1 \times 10^5$ cells/well (50 μl). NMs (Ag, $TiO_2$, MWCNTs, ZnO) were added (50 μl) to wells in triplicate to give final NM concentrations of 1.9–125 μg/ml (equivalent to 0.03–2 μg/$cm^2$). The toxicity of the dispersant for Ag NM toxicity was also investigated. The toxicity of ufCB to HL60 cells has been tested previously (Brown et al., 2010) thus only a limited number of concentrations (15 and 31 μg/ml) were tested to confirm that the concentrations selected were not cytotoxic. Triton-X100 (0.1%) was used as a positive control for cytotoxicity. After 24 h the cell supernatant was removed and stored at −80 °C and cell viability was assessed using the alamar blue assay (resazurin sodium salt 0.01 mg/ml, in complete cell culture medium). Cell fluorescence was measured at a wavelength of 560/590 nm (excitation/emission). The data are expressed as a percentage of the negative control (i.e. % viability). To check for NM interference in the assay fluorescence was measured in treated cells prior to the addition of the alamar blue reagent, and a fluorescence reading was taken following NM incubation with the alamar blue reagent in the absence of cells. The results obtained from cytotoxicity testing were used to rank the toxicity of the NM panel tested. Ag, and ZnO NMs exhibited high toxicity, and MWCNTs, $TiO_2$ and ufCB exhibited low toxicity. Three NMs (Ag, $TiO_2$ and ufCB) were selected for a more in depth assessment of their toxicity.

### 2.4. Cytokine production

A pilot study was conducted to identify what cytokines should be analysed following exposure of cells to NMs. Cell supernatants generated during the cytotoxicity tests were used for this cytokine analysis. Only one concentration of each NM type was analysed in the pilot study, and the production of TNFα, IL-8, MCP-1, IL-6, and IL-10 was assessed using a BD Biosciences cytometric bead array flex set kit (Becton Dickinson supplier, Oxford, UK). These studies demonstrated that only MCP-1 and IL-8 were increased in response to NM exposure (data not shown). The dose and time dependency of cytokine production was then investigated for these cytokines. Cells were differentiated as described previously and plated at a concentration of $1 \times 10^5$ cells/well (50 μl) into 96 well plates and exposed to NMs (Ag, $TiO_2$ or ufCB) (50 μl) in triplicate for 4 or 24 h. Limited (sub-lethal) concentrations of NMs were included. Three concentrations of Ag NM were selected that were equivalent to the $LC_{20}$ concentration (the concentration of NM required to kill 20% of cells), ½ the $LC_{20}$ concentration and double $LC_{20}$ concentration, which equated to 3.9, 7.8 and 15.6 μg/ml respectively. The $LC_{20}$ was not reached for $TiO_2$ and ufCB NMs, and so concentrations of 15.6, 31.25, 62.5 μg/ml were selected. Following exposure to the NM panel, the cell supernatant was frozen at −80 °C, until the cytokine analysis was performed using a BD Biosciences cytometric bead array flex set kit.

### 2.5. Impact of inhibitors of $Ca^{2+}$ signaling and the antioxidant trolox on Ag NM mediated cytokine production

Cells were differentiated as described above, seeded at a concentration of $2 \times 10^6$ cells/ml (50 μl) into 96 well plates. Cells were then exposed to Ag NMs (7.8 μg/ml, 50 μl) and either 1,2-Bis(2-aminophenoxy)ethane-N,N,N′,N′-tetraacetic acid tetrakis (acetoxymethyl ester) (BAPTA-AM, 1 μM), verapamil (12.5 μM), or 1-[2-(4-Methoxyphenyl)-2-[3-(4-methoxyphenyl)propoxy]ethyl]imidazole,1-[β-(3-(4-Methoxyphenyl)propoxy)-4-ethoxyphenethyl]-1H-imidazole hydrochloride (SKF96365, 5 μM) for 4 h. Alternatively, cells were pre-treated with trolox (25 μM) for one hour, washed and then exposed to Ag NMs (7.8 μg/ml) for 4 h. Following treatment the cell supernatant was frozen at −80 °C, until the cytokine analysis was performed using a BD Biosciences cytometric bead array flex set kit.

### 2.6. Impact of NMs on $Ca^{2+}$ signaling

Cells were differentiated and NMs were dispersed as described above, however, following sonication NMs were diluted in serum-free RPMI medium containing 10 mM HEPES. Intracellular $Ca^{2+}$ concentration was measured using the fluorescent probe Fura-2 as described previously (Brown et al., 2010). Sub-lethal concentrations of each type of NM under investigation were selected, according to the results from the cytotoxicity testing. As the NMs being tested varied in their potency, different concentrations were used for each NM, when assessing their impact on intracellular $Ca^{2+}$ concentration. Cells were exposed to a final concentration of 1.9 or 3.9 μg/ml Ag NMs, 15 or 31 μg/ml ufCB and 31 μg/ml $TiO_2$. Cells were exposed to the appropriate NM treatment or control (serum-free RPMI medium containing 10 mM HEPES) for 1000 s. The average intracellular $Ca^{2+}$ concentration was calculated during the first 100 s of treatment and last 100 s of treatment. To check for NM interference, the experiment was performed for each NM in the absence of cells.

Differentiated HL60 cells were also seeded at a concentration of $1 \times 10^6$ cells/ml in 35 mm Petri dishes (1 ml). After 24 h cells were washed with electrophysiology buffer (140 mM NaCl, 4 mM KCl, 1.8 mM $CaCl_2$, 1 mM $MgCl_2$, 10 mM HEPES, 10 mM Glucose, pH

7.4). Electrophysiology buffer (1 ml) was added to cells following washing and the cells were observed to loosely adhere to the Petri dish surface overnight. Cells were identified by light microscopy and then subjected to whole-cell voltage clamp using a HEKA EPC7 amplifier. Data were acquired using 'Clampex' and was analysed using Clampfit (Molecular Devices, LLCCA, United States, version 10.3). Recordings were conducted at 18–20 °C using $AgCl_2$ electrodes and filamented borosilicate glass patch pipettes with resistances of 3–7 MΩ. The bath solution contained the electrophysiology buffer (described above) and the pipette solution contained; 150 mM CsCl, 20 mM KCl, 1 mM $CaCl_2$, 1 mM $MgCl_2$, 10 mM HEPES, 3 mM Phosphocreatine Na, 11 mM ethylene glycol-bis(2-aminoethylether)-N,N,N′,N′-tetraacetic acid, 9 mM D (+)-Sucrose, 4 mM ATP-$Mg_2$; pH 7.2; 295 mOsm/kg. Cells were judged suitable for recording if the holding current at −60 mV was less than −100 pA (not less than 0.6 GΩ). A baseline recording of membrane current was made for at least 2 min to establish stability, then NMs were pipetted directly into the Petri dish (50 μl) to obtain final concentrations of 1.9 or 3.9 μg/ml for Ag NMs, and 31 μg/ml for ufCB and $TiO_2$ NMs. The membrane current was measured (in voltage clamped cells) over a 20 min observation time.

### 2.7. Superoxide anion production

Changes in cytochrome c reduction following exposure to NMs were used to monitor changes in superoxide anion production as an indicator of the respiratory burst. Differentiated cells were adjusted to a cell concentration of $5 \times 10^6$ cells/ml. The cell suspension ($2.5 \times 10^5$ cells/well) or complete cell culture medium (50 μl) or the test substance (50 μl) was then added to a 24 well plate. Sub-lethal concentrations of each type of NM under investigation were selected to investigate superoxide production. As the NMs being tested varied in their potency, different concentrations were used for each NM. NMs were prepared and sonicated as described above. NMs were then diluted in complete cell culture medium to give a final concentration of 0.49, 0.98, 1.95 or 3.9 μg/ml for Ag, or 7.8, 15.6, 31.25 μg/ml for $TiO_2$ and ufCB. Experiments were conducted in the absence and presence of cells to account for NM interference in the assay and NM mediated production of ROS in the absence of cells. A volume of 900 μl of the reaction mixture (80 μM cytochrome c, and 11 mM dextrose, in PBS) was added to each well. Phorbol myristate acetate (PMA, 0.01 μg/ml) was used as a positive control to induce a respiratory burst. Two hours post exposure samples were transferred to a 96 well plate in triplicate groups (100 μl) and absorbance read at 488 nm and 550 nm. The level of superoxide production was calculated in the presence and absence of cells and data expressed as nMoles of superoxide/ml.

### 2.8. Apoptosis induced by NMs

Differentiated HL60 cells were adjusted to a cell concentration of $0.5 \times 10^4$ cells/well (50 μl) and exposed to either complete cell culture medium (control), staurosporine (2.5 μM, positive control), Ag (1.9, 3.9, 7.8 and 15.6 μg/ml), $TiO_2$ (15.6, 31.25, or 125 μg/ml) or ufCB (15.6, 31.25, or 125 μg/ml) NMs (50 μl) in a 96 well plate for 24 h. The number of apoptotic cells was evaluated using the BD Pharmingen PE Annexin V apoptosis detection kit and apoptotic cells measuring using BD FACS Array. Cyto-centrifuge preparations of the cell suspension for the control cells and cells exposed to a concentration of 15.6 μg/ml Ag NMs or 125 μg/ml of either $TiO_2$ or ufCB were also prepared in tandem with the Annexin V apoptosis detection kit; these were fixed with methanol and stained with Rapid Romanowsky stain then viable and apoptotic cells were visualised using light microscopy.

### 2.9. Statistical analysis

All experiments were performed at least three times, on three separate days. All data are expressed as mean ± standard error of the mean (SEM). For statistical analysis an ANOVA General Linear Model was performed followed by a post hoc Tukeys test using Minitab 15. A $p$ value of <0.05 was considered to be a significant finding.

## 3. Results

### 3.1. Physico-chemical characterisation

The hydrodynamic diameter, zeta potential and polydispersity index (PdI) of NMs suspended in complete cell culture medium was measured using DLS (Table 2). MWCNTs could not be measured as DLS analysis is not applicable to non-spherical NMs. Ag, TiO2, ZnO and ufCB NMs were agglomerated in cell culture medium, to varying extents. When the primary particle size of all NMs was taken into consideration (Table 1) it was evident that $TiO_2$ and ufCB NMs were the most agglomerated NM tested, and that Ag and ZnO NMs were the least agglomerated NMs. All NMs had a negative zeta potential. The PdI values (measure of the broadness of the size distribution) for all NMs were <1, indicating that all samples were suitable for DLS analysis.

### 3.2. Impact of NMs on cell viability

Differentiated HL60 cell viability decreased in a dose dependent manner following exposure to ZnO, Ag and MWCNT NMs for 24 h (Fig. 1). $TiO_2$ NMs did not affect cell viability at any of the concentrations tested (Fig. 1). In contrast, Ag was the most toxic NM tested, causing a significant decrease in cell viability at concentrations of 15.6 μg/ml and higher, when compared to the control. More specifically, cell viability was reduced to 35% in cells following exposure to 15 μg/ml Ag NM, and 13% of cells were viable when exposed to concentrations of Ag NM greater than 31.25 μg/ml. ZnO NMs also induced a significant decrease in cell viability, but at slightly greater concentrations of 31.25 μg/ml and higher, when compared to the control. At a concentration of 31.25 μg/ml ZnO NM cell viability was reduced to 39%, and was 22% at a concentration of 125 μg/ml. MWCNTs stimulated a significant reduction in cell viability to 55% only at the highest concentration tested (125 μg/ml). The lethal concentration $(LC)_{50}$ (concentration of NM required to kill 50% of cells) was 13 μg/ml for Ag NMs and 17 μg/ml for ZnO NMs. The $LC_{50}$ for $TiO_2$ NMs and MWCNTs was not reached. The toxicity of ufCB particles to HL60 cells has been tested previously (Brown et al., 2010), therefore a full dose response experiment was not conducted for this NM type. Instead only limited concentrations (15 and 31 μg/ml) of ufCB were tested to confirm that these NM concentrations were not associated with cytotoxicity (data not shown). The Ag NMs were supplied in a suspension, and the toxicity of this dispersant was assessed. No cytotoxicity was associated with the Ag NM dispersant (data not shown). Information from the cytotoxicity

**Table 2**
Hydrodynamic diameter, zeta potential and PdI of NM panel when dispersed in complete cell culture medium (31 μg/ml). Data expressed as mean ± SEM ($n$ = 3).

| NM | Hydrodynamic diameter (nm) | Zeta potential (mV) | PdI |
|---|---|---|---|
| $TiO_2$ | 635.4 ± 22.5 | −8.2 ± 0.09 | 0.458 ± 0.02 |
| Ag | 77.93 ± 1.2 | −8.9 ± 0.52 | 0.459 ± 0.004 |
| ZnO | 325.2 ± 29.9 | −7.61 ± 1.3 | 0.389 ± 0.09 |
| ufCB | 238.2 ± 18.9 | −8.1 ± 7 | 0.601 ± 0.1 |

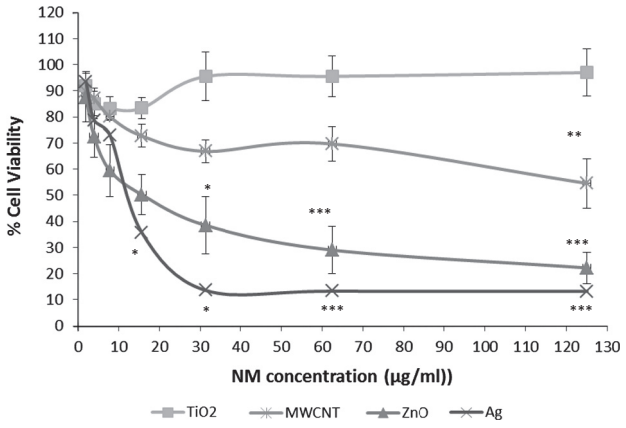


**Fig. 1.** Viability of differentiated HL-60 cells following NM exposure. Cells were exposed to either complete cell culture medium (control), $TiO_2$, MWCNT, ZnO or Ag NMs at concentrations ranging from 1.9 µg/ml to 125 µg/ml for 24 h. The viability of cells was assessed using the alamar blue assay. The data are expressed as the average percentage of cell viability (i.e. % of the control) ± SEM ($n = 3$). Significance indicated by * = $p < 0.05$, ** = $p < 0.01$, and *** = $p < 0.001$.

analysis was used to rank the toxicity of the NMs and thereby prioritise the selection of NMs for mechanistic studies, and to identify sub-lethal concentrations of NM to test within these studies. ZnO and Ag NMs were found to be of relatively high toxicity, whereas $TiO_2$ and MWCNTs found to be of low toxicity. Thus Ag (a high toxicity NM), $TiO_2$ (a low toxicity NM) were selected to perform a more comprehensive toxicity assessment. ufCB was also included as data exist on the mechanism of pro-inflammatory mediator production via ROS and $Ca^{2+}$ signaling in macrophages (Brown et al., 2004a,b), as well as data in the HL60 cells showing an ability to induce $Ca^{2+}$ influx (Brown et al., 2010).

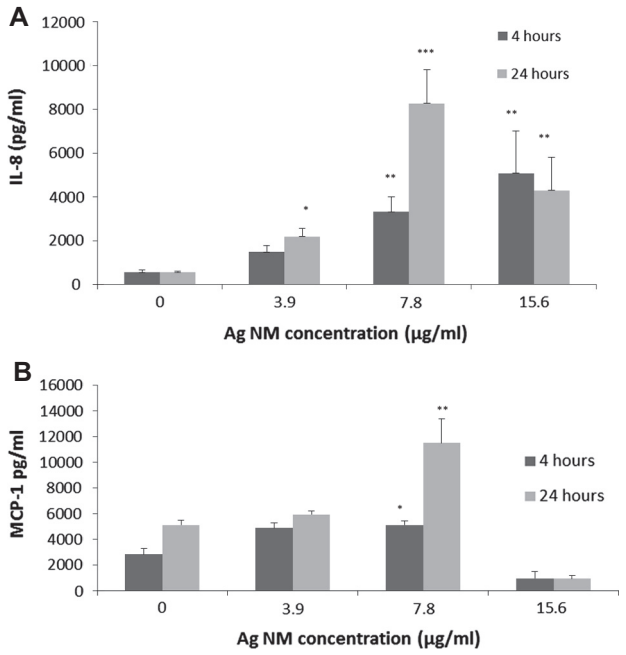


**Fig. 2.** Cytokine production by differentiated HL60 cells following NM exposure. Cells were exposed to complete cell culture medium (control, 0), or Ag NMs at concentrations of 3.9, 7.8, and 15 µg/ml for 4 or 24 h. The level of and IL-8 (A) and MCP-1 (B) in the cell supernatant was analysed using a BD Biosciences cytometric bead array flex set kit. The data are expressed as the average level of cytokine production (pg/ml) ± SEM ($n = 3$). Significance indicated by * = $p < 0.05$, ** = $p < 0.01$, and *** = $p < 0.001$.

### 3.3. NM mediated cytokine production

Ag NMs induced a time and dose dependent increase in MCP-1 and IL-8 cytokine production by cells. A significant increase in IL-8 production was observed at Ag NM concentrations of 7.8 and 15.6 µg/ml, 4 h post exposure, and at concentrations of 3.9, 7.8 and 15.6 µg/ml 24 h post exposure, when compared to the control (Fig. 2A). A significant increase in MCP-1 production was observed at a concentration of 7.8 µg/ml, 4 and 24 h post exposure when compared to the control (Fig. 2B). No change in cytokine production was observed in response to ufCB and $TiO_2$ NM exposure at the concentrations tested (data not shown).

### 3.4. Cytokine production following exposure of Ag NM exposed cells to $Ca^{2+}$ signaling inhibitors or the antioxidant Trolox

Cytokine production was evaluated following a 4 h co-exposure of cells to Ag NMs (7.8 µg/ml) and inhibitors of $Ca^{2+}$ signaling; either BAPTA-AM (a chelator of intracellular $Ca^{2+}$ stores), verapamil (plasma membrane $Ca^{2+}$ channel blocker) or SKF96365 (depletes intracellular store of $Ca^{2+}$). This work aimed to identify the contribution of $Ca^{2+}$ signaling to induction of Ag NM mediated cytokine production by cells. In addition, the impact of trolox (antioxidant) pre-treatment was evaluated to determine the contribution of ROS production to Ag NM mediated cytokine production by cells. Following exposure to Ag NMs a significant increase in IL-8 (Fig. 3A) or MCP-1 (Fig. 3B) production was observed, when compared to the unstimulated control. BAPTA-AM, verapamil, and SKF96365 prevented the Ag NM mediated increase in IL-8 and MCP-1 production (Fig. 3A and B). Similarly, a pre-treatment of

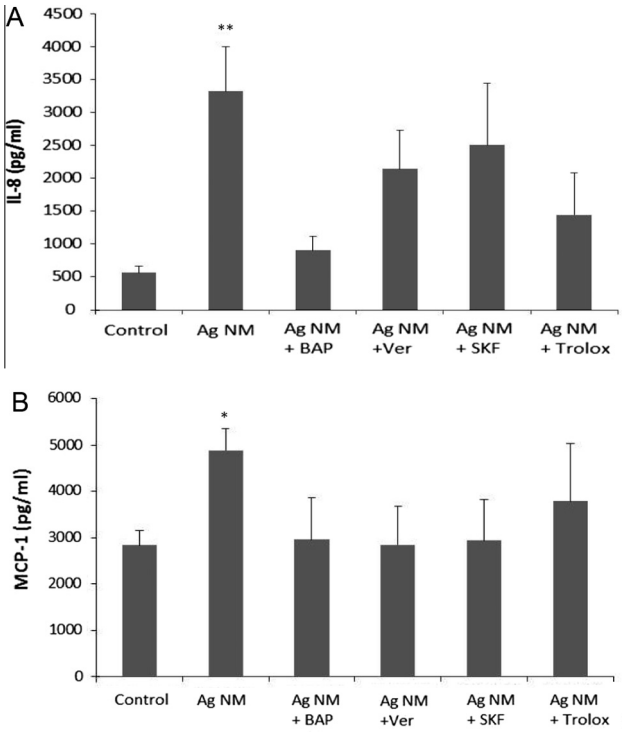


**Fig. 3.** Cytokine production by differentiated HL60 cells following co-exposure to NMs and inhibitors of Ca2+ or the antioxidant Trolox. Cells were exposed to complete cell culture medium (control), or Ag NMs at a concentration of 7.8 µg/ml for 4 h. A co-exposure to Ag NMs and either BAPTA-AM (BAP, 1 µM), Verapamil (Ver, 12.5 µM), or SKF96365 (SKF, 5 µM) or following a 1 h pre-treatment of cells with Trolox (25 µM) was conducted for 4 h. The level of IL-8 (A) and MCP-1 (B) in the cell supernatant was then analysed using a BD Biosciences cytometric bead array flex set kit. The data are expressed as the average level of cytokine production (pg/ml) ± SEM ($n = 3$). Significance indicated by * = $p < 0.05$, and ** = $p < 0.01$.

cells with trolox was prevented the increase in IL-8 or MCP-1 production mediated by Ag NMs (Fig. 3A and B).

### 3.5. Superoxide anion production (respiratory burst)

Ag NMs stimulated a dose dependent increase in superoxide production 2 h post exposure (Fig. 4). A significant elevation in superoxide anion production was observed at a concentration of 3.9 μg/ml Ag NM, when compared to the control (Fig. 4). $TiO_2$ and ufCB NMs did not impact on superoxide anion production by cells at any of the concentrations tested (data not shown).

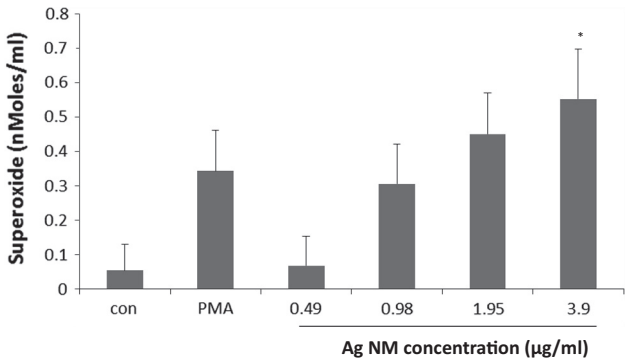


**Fig. 4.** Superoxide anion production by differentiated HL-60 cells following NM exposure. Cells were exposed to complete cell culture medium (control), PMA (0.01 μg/ml) (positive control), or Ag NMs at concentrations of 0.49, 0.98, 1.95 and 3.9 μg/ml for 2 h. The level of superoxide production was then analysed using the cytochrome c assay. The data are expressed as average level of superoxide anion production (nMoles/ml) ± SEM ($n = 3$). Significance indicated by * = $p < 0.05$.

### 3.6. Intracellular $Ca^{2+}$ concentration

Differentiated HL-60 cells loaded with the fluorescent probe Fura-2 were exposed to NMs for 1000 s, and the intracellular $Ca^{2+}$ concentration ($[Ca^{2+}]_i$) measured throughout the observation. The average $[Ca^{2+}]_i$ over the first and the last 100 s of the treatment time was calculated following NM exposure. $TiO_2$ NMs did not stimulate an increase in $[Ca^{2+}]_i$, when compared to the control (Fig. 5A and B). Ag and ufCB NMs stimulated a dose and time dependent increase in $[Ca^{2+}]_i$ in cells (Fig. 5A and B). A significant elevation in $[Ca^{2+}]_i$ was observed during the last 100 s of the treatment following exposure to Ag NMs at a concentration of 3.9 μg/ml (Fig. 5B). ufCB NMs stimulated a significant increase in $[Ca^{2+}]_i$ at a concentration of 31 μg/ml during the first and last 100 s of the treatment, when compared to the control (Fig. 5A and B).

Whole cell voltage clamping of cells was carried out to investigate the origin of the rise in $[Ca^{2+}]_i$. Control cells were stable during the observation time of 20 min (Fig. 6A). At a concentration of 3.9 μg/ml Ag NMs induced a prominent inward ionic current 2–5 min after the addition of Ag NMs (Fig. 6A). A steady increase in membrane current and membrane noise was then observed over the rest of the observation time (Fig. 6A). The effect of Ag NMs on membrane current was irreversible as washing did not adjust

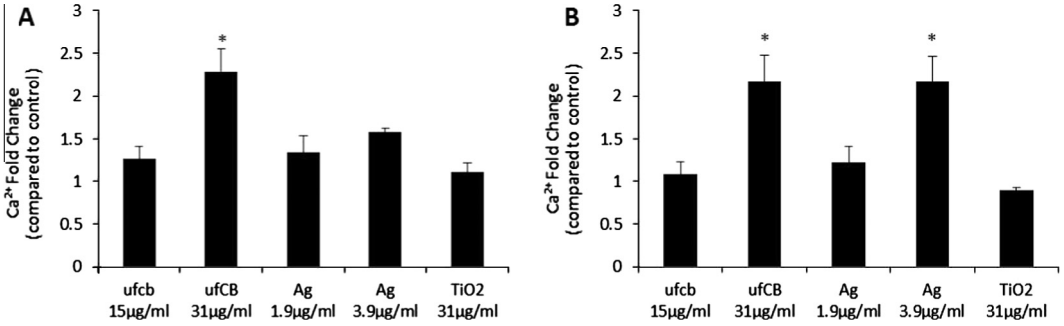


**Fig. 5.** Intracellular $Ca^{2+}$ concentration in differentiated HL-60 cells following exposure to NMs. Following differentiation, the HL60 cell line was exposed to Ag (1.9 and 3.9 μg/ml), $TiO_2$ (31.25 μg/ml) or ufCB (15 and 31 μg/ml) NMs (in serum-free RPMI medium containing 10 mM HEPES) for 1000 s. The level of intracellular $Ca^{2+}$ was monitored using the fluorescent probe Fura-2 during the observation time. The data are expressed as the average fold change in $Ca^{2+}$ concentration compared to the control ± SEM (n = 3) during the first 100 s of the 1000 s treatment (A), and last 100 s of the 1000s treatment (B). Significance indicated by * = $p < 0.05$.

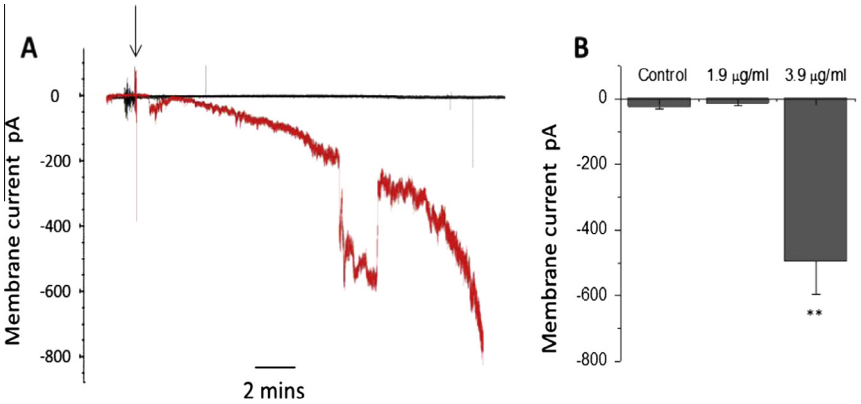


**Fig. 6.** Changes in membrane ion current in differentiated HL-60 cells following Ag NM exposure. Example recordings from control (black trace), and Ag NM (3.9 μg/ml) exposed (red trace) cells (A). Control treatment (electrophysiology buffer) or Ag NMs (3.9 μg/ml) were added at the downward pointing arrow, and changes in membrane current monitored over a 20 min observation time. The mean inward membrane current observed following exposure to Ag NMs or electrophysiology buffer (control) was calculated (B). Error bars represent the Standard Error of the mean (S.E.M). Significance indicated by ** = $p < 0.01$.

the current flow back to control levels (data not shown). At a concentration of 1.9 μg/ml, Ag NMs did not induce a change in ion current in cells (Fig. 6B). $TiO_2$ NMs and ufCB did not induce an inward ion current when tested at a concentration of 31 μg/ml (data not shown).

### 3.7. Apoptosis

A significant increase in the percentage of apoptotic cells was evident following Ag NM exposure at a concentration of 15.6 μg/ml, 24 h post exposure (Fig. 7). $TiO_2$ and ufCB NMs were not able to induce apoptosis in cells at any of the concentrations tested 24 h post exposure (Fig. 7). Light microscopy was used to visualise cell morphology following exposure to NMs to further investigate their ability to induce apoptosis. It was observed from cyto-centrifuge preparations that cells exposed to $TiO_2$ or ufCB (125 μg/ml) had a similar appearance to control cells indicating that the cells were viable following exposure to these NMs (Fig. 8). However, cells exposed to Ag NMs (15.6 μg/ml) appeared to be apoptotic due to their shrunken and unhealthy appearance (Fig. 8).

### 3.8. Cell activation

The appearance of cells following exposure to the NM panel was visualised using light microscopy 2 h post exposure (Fig. 9). From

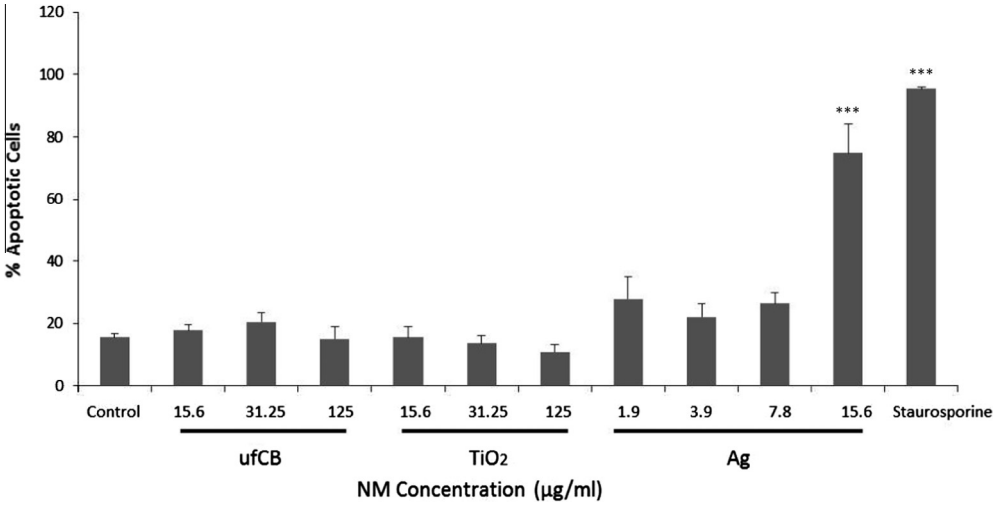


**Fig. 7.** Apoptosis induced by NMs in differentiated HL-60 cells. Cells were exposed to complete cell culture medium (control), staurosporine (2.5 μM, positive control), Ag NMs (1.9, 3.9, 7.8 and 15.6 μg/ml), $TiO_2$ NMs (15.6, 31.25, or 125 μg/ml) or ufCB (15.6, 31.25, or 125 μg/ml) for 24 h. The number of apoptotic cells was measured using the BD Pharmingen PE Annexin V apoptosis detection kit and the samples analysed using FACS Array. The data are expressed as the percentage of apoptotic cells ± SEM ($n = 3$). Significance indicated by *** = $p < 0.001$.

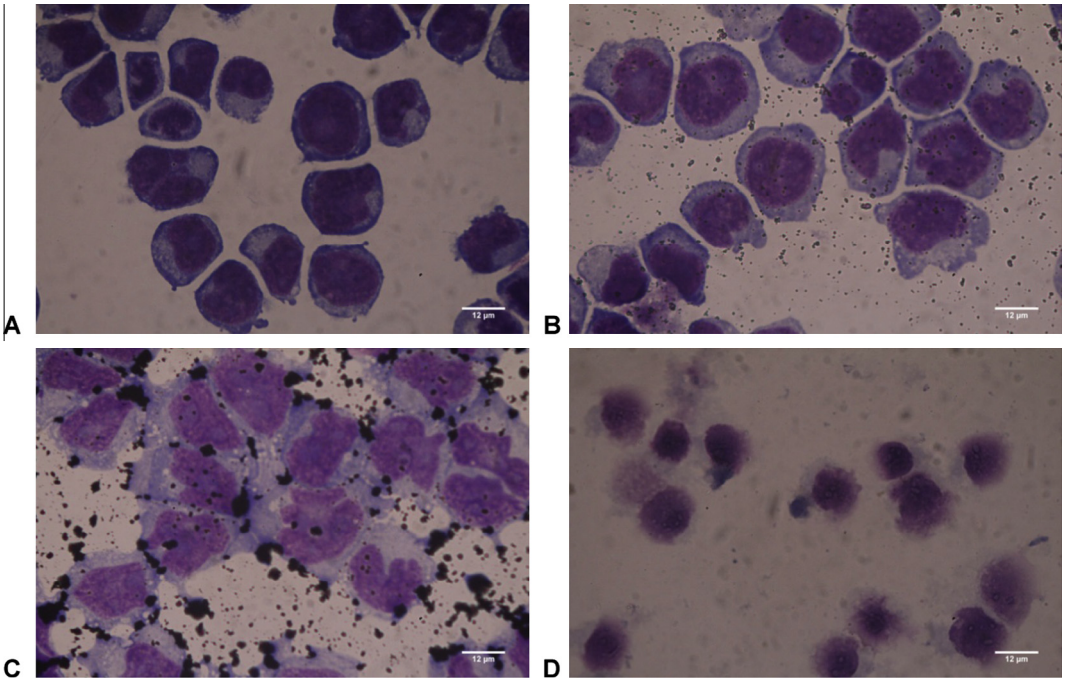


**Fig. 8.** Differentiated HL-60 cell viability following exposure to NMs. Cells were exposed to complete cell culture medium (control, A), 125 μg/ml $TiO_2$ NMs (B), 125 μg/ml ufCB (C) 15.6 μg/ml Ag NMs (D) for 24 h. The cells were fixed and stained then observed using light microscopy (magnification 1000×), scale bar = 12 μm.

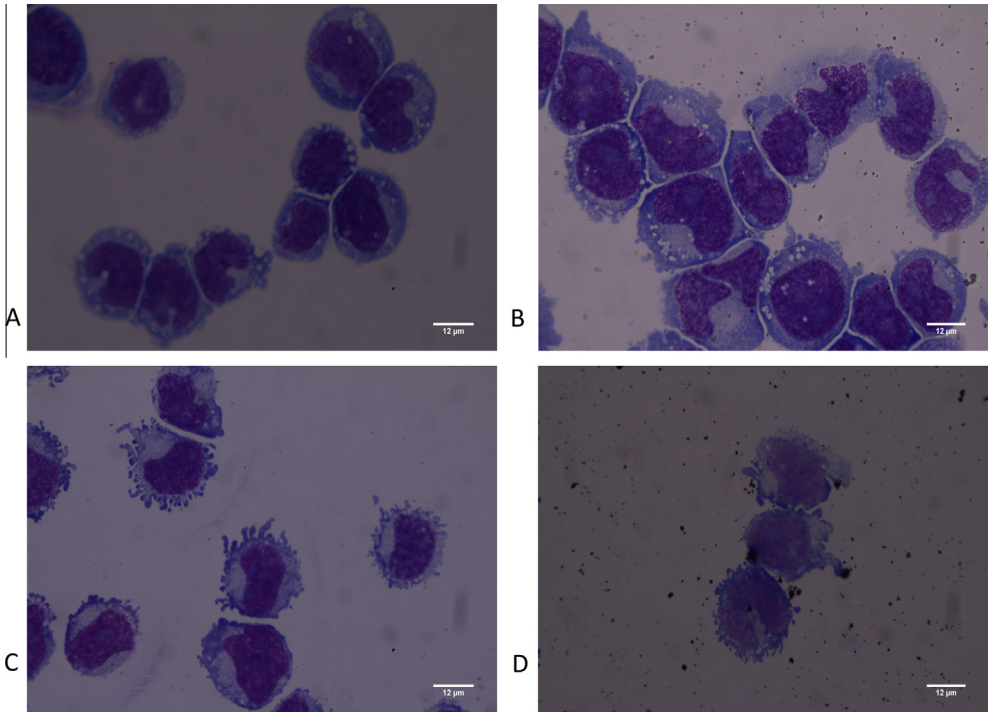


**Fig. 9.** Cell activation following exposure to NMs. Differentiated HL60 cells were exposed to complete cell culture medium (control, A), 31 µg/ml $TIO_2$ NMs (B), 31 µg/ml ufCB (C) 3.9 µg/ml Ag NMs (D) for 2 h. The cells were washed, fixed and stained and observed using light microscopy (magnification 1000×), scale bar = 12 µm.

analysis of cyto-centrifuge preparations, the control cells, and cells exposed to $TiO_2$ NMs had a similar appearance (Fig. 9A and B). The morphology of cells changed following exposure to ufCB and Ag NMs which was indicative that they had become activated (Fig. 9C and D). More specifically, cells exhibited membrane ruffling consistent with an activated phenotype.

## 4. Discussion

This study aimed to determine the mechanism underlying the response of differentiated HL60 cells to NMs of varied physico-chemical properties. A focus was placed on investigating the involvement of $Ca^{2+}$ and oxidant signaling to the cellular response stimulated by NMs. A panel of NMs was initially selected for investigation in this study, namely; Ag, $TiO_2$, MWCNTs, and ZnO. The panel was chosen on the basis that there is considerable information available on the toxicity of these exact NMs both *in vivo* (e.g. Kermanizadeh et al., 2013a) and *in vitro* (e.g. Kermanizadeh et al., 2013b, 2013c) at different cell and tissue targets (e.g. lung, liver, kidney, macrophages). Investigation of the capacity of the NM panel to induce cytotoxicity was performed in the first instance to identify sub-lethal concentrations of NMs to test in more in depth mechanistic studies, and to contribute to the ranking of the hazard potential of NMs. This enabled us to identify selected NMs (namely Ag and $TiO_2$) to test when assessing the cellular and molecular mechanism by which NMs induce neutrophil activation. The response of neutrophils, and an in depth investigation of the mode of action by which NM types exhibit toxicity to neutrophils or other cell types has not been evaluated previously. This study used differentiated HL60 neutrophil-like cells which allows comparison of the response of this cell model to other cell types to investigate differences in cell sensitivity, and provides the opportunity to investigate the cellular and molecular response to the NMs tested in this study to better understand the mechanism underlying observed toxicity. Such an understanding is critical for the urgent requirement to develop appropriate alternative and intelligent testing strategies for NM hazard/risk assessment (Stone et al., 2014).

The ability of NMs to induce oxidative stress is frequently investigated when assessing the toxicity posed by NMs to mammalian cells, rodent models, bacteria, and environmental organisms (e.g. Ali et al., 2014; Brown et al., 2001; Gomes et al., 2014; Kermanizadeh, 2013b,c; Shvedova et al., 2007). As such, oxidative stress based assays are now a routine consideration in hazard assessments for NMs. Oxidative stress is hypothesised to drive the inflammogenicity and carcinogenicity of inhaled pathogenic particles (e.g. particulate air pollution particles) and therefore their propensity to stimulate adverse health effects (for reviews please refer to Li et al., 2008; Nel et al., 2006; Risom et al., 2005). Only limited studies have investigated the relationship between NM exposure, oxidative stress and pro-inflammatory responses (e.g. McCarthy et al., 2012). Instead, studies to date have focused on investigating the contribution of oxidative stress to NM mediated genotoxicity (e.g. Akhtar et al., 2013; Ahamed et al., 2013; Gerloff et al., 2011; Kim et al., 2011; Monteiller et al., 2007; Sharma et al., 2011; Shukla et al., 2011; Tarantini et al., 2014). In fact, it is likely that NMs induce a tiered response that is dependent on the NM exposure concentration and therefore level of oxidative stress that is induced in cells. 'Low' levels of oxidative stress activate cytoprotective responses, and at 'higher' levels more damaging responses are stimulated (e.g. pro-inflammatory responses, genotoxicity, cell death) which require the activation of different intracellular signaling cascades (Brown et al., 2004a, 2010; Li et al., 2002, 2008; Nel et al., 2006). In addition, very little literature is available on the ability of NMs to induce $Ca^{2+}$ signaling, the nature of $Ca^{2+}$ signaling and the consequences of this signaling, or the role of NM mediated oxidant production in inducing this signaling, despite its known contribution to the toxicity of other pathogenic particles (e.g. Brown et al., 2004a). Therefore, whilst hazard studies for NMs commonly investigate an array of cell responses (e.g. cytotoxicity, pro-inflammatory effects, genotoxicity) (e.g. Suliman et al., 2013; Tarantini et al., 2014) they do not often investigate

the relationship between these processes (e.g. activation of $Ca^{2+}$ and oxidant based signaling pathways, and subsequent activation of transcription factors). This manuscript therefore provides information that contributes to addressing these data gaps.

Of the panel of NMs tested Ag NMs were consistently observed to be the most potent activator of cells with respect to the cellular and molecular responses investigated in the study. Within minutes of exposure, Ag NMs (3.9 μg/ml) induced an inward membrane ion current and a rise in intracellular $Ca^{2+}$ concentration. At 2 h, Ag NMs (3.9 μg/ml) stimulated a respiratory burst (superoxide production), while at 4 h Ag NMs (>3.9 μg/ml) stimulated cytokine production (IL-8 and MCP-1) via a mechanism involving $Ca^{2+}$ and oxidant signaling. This cytokine response was retained at 24 h. Cell death (via apoptosis) was detected at 24 h at Ag NM concentrations >15.8 μg/ml. This diverse range of observations adds important detail to both the time course and mode of action of the Ag NM mediated toxicity to HL60 cells; namely the role of $Ca^{2+}$ and oxidative stress in cell responsiveness (Figs. 10 and 11).

Interestingly, in this study ufCB was able to stimulate an increase in intracellular $Ca^{2+}$ concentration (31 μg/ml) within minutes of exposure and to induce a change in cell morphology that was indicative of cell activation. However no changes in cytokine or superoxide production were observed, suggesting that this NM acts via a different mode of action to Ag NMs. In contrast, $TiO_2$ did not impact on any of the parameters assessed, and as a consequence was defined as being relatively non-toxic.

If a single assay (e.g. assessment of intracellular $Ca^{2+}$ concentration) had been used to screen NM toxicity it would have been difficult to obtain a comprehensive overview of NM toxicity or biological potency that would allow evidence based ranking of hazard. As a consequence of the range of endpoints chosen it was relatively easy to rank the toxicity of NMs as Ag > ufCB > $TiO_2$. The information obtained regarding the mode of action of NM toxicity could therefore be developed further to form evidence based approaches to guide research activities which screen the toxicity of a wider range of NMs to other cell types in the future.

### 4.1. NM mediated changes in intracellular $Ca^{2+}$ concentration

$Ca^{2+}$ is a second messenger molecule that is responsible for controlling a spectrum of cell functions in excitable and non-excitable cells (Takahashi et al., 1999; Trump and Berezesky, 1995). In fact, one of the first events in neutrophil activation is an increase in $[Ca^{2+}]_i$ (O'Flaherty et al., 1991; Tintinger et al., 2005). Due to its importance to normal cell function $[Ca^{2+}]_i$ is tightly regulated. There is evidence that NMs are able to exert toxicity by modulating $[Ca^{2+}]_i$. For example ufCB stimulates an increase in $[Ca^{2+}]_i$ in macrophages (Stone et al., 2000; Brown et al., 2000, 2004a, 2004b), and neutrophils (Brown et al., 2010). Increases in $[Ca^{2+}]_i$ mediated by ufCB have implications for macrophage cell function including increased cytokine production (Brown et al., 2004a,b) and cytoskeletal dysfunction (Möller et al., 2005). The pro-inflammatory responses stimulated by NMs have been extensively investigated at a variety of target sites using *in vitro* and *in vivo* models to investigate NM hazard. However, the role of $Ca^{2+}$ in the cell response to NMs has been neglected in recent years.

In this study changes in $[Ca^{2+}]_i$ were investigated following the exposure of Fura-2 loaded neutrophil-like HL-60 cells to sub-lethal concentrations of NMs. Ag NMs and ufCB stimulated an increase in $[Ca^{2+}]_i$. For Ag NMs these changes were related to cell activation (i.e. cytokine and ROS production). The majority of previous studies have investigated the impact of NMs on $[Ca^{2+}]_i$ in relation to cell viability (Schaeublin et al., 2011; Bhattacharjee et al., 2013; Xia et al., 2006; Luo et al., 2012; Huang et al., 2010). However as $Ca^{2+}$ controls a host of cell functions we considered the sub-lethal impacts of raised $[Ca^{2+}]_i$ following NM exposure.

To investigate the origin of the $[Ca^{2+}]_i$ rise mediated by Ag NMs, whole cell voltage clamping of cells was performed. This approach revealed that Ag NMs generate a concentration dependent inward ionic current within a few minutes of exposure. The change in membrane current observed could be carried by an inward $Ca^{2+}$ and/or $Na^+$ current. We suggest that this would generate an increase in $[Ca^{2+}]_i$ either by depolarizing the cells or by direct influx of $Ca^{2+}$. Further work on the ionic selectivity of the membrane under these conditions could determine the species of ions that are generating the current.

The mechanism by which $Ca^{2+}$ enters cells following exposure to NMs was not investigated in this study. Voltage clamp experiments (data not shown) failed to reveal active voltage sensitive $Ca^{2+}$ or $Na^+$ currents in the HL60 cells, confirming existing work showing that only voltage operated $K^+$ and $Cl^-$ channels are present in neutrophils (Krause and Welsh, 1990). The predominant route of $Ca^{2+}$ influx into non-excitable cells such as neutrophils is through the opening of plasma membrane store operated $Ca^{2+}$ channels in response to the emptying of intracellular $Ca^{2+}$ stores which is termed store operated $Ca^{2+}$ entry (SOCE) (Bréchard and Tschirhart, 2008). There is also evidence that oxidative stress and $Ca^{2+}$ signaling are intimately linked (Ermak and Davies, 2002). For example, previous studies have demonstrated that oxidative stress stimulates the rise in $Ca^{2+}$ concentration observed in response to NMs in macrophages (Stone et al., 2000; Brown et al., 2004a,b; Xia et al., 2006; Huang et al., 2010). In addition, it is

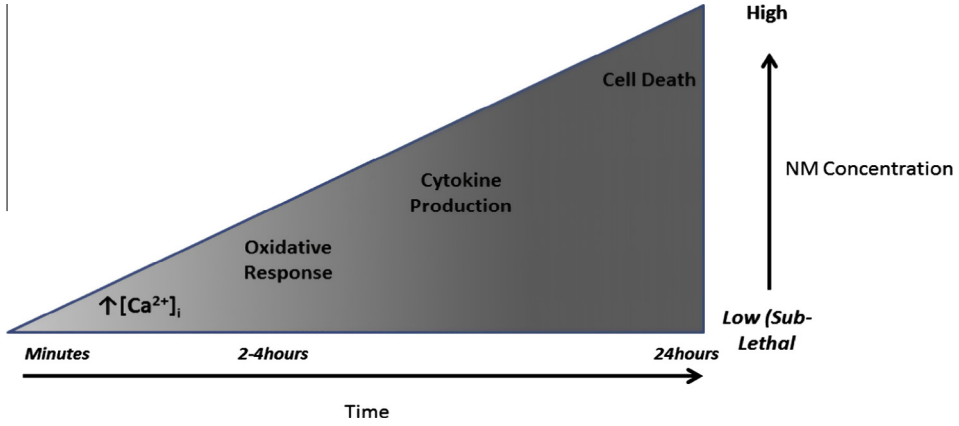


**Fig. 10.** Mechanism of Ag NM mediated toxicity to differentiated HL60 cells. Within minutes of exposure an influx of $Ca^{2+}$ into the cell is observed. Oxidative responses (encompassing intracellular ROS production, oxidative signaling and a respiratory burst) are then stimulated within 4 h of exposure. Cytokine production is observed at 4 and 24 h post-exposure. The capacity of Ag NMs to stimulate cell death 24 h post exposure is dictated by the NM concentration.

also possible that NMs cause the formation of small pores in the plasma membrane of cells to enable the entry of $Ca^{2+}$ into the cell interior from the extracellular environment. If NMs make the membrane permeable to ions via this mechanism $Ca^{2+}$ and $Na^{+}$ would move down their concentration gradients towards equilibrium (e.g. $Ca^{2+}$ moves from the extracellular environment to the cell interior).

Investigation of $[Ca^{2+}]_i$ following exposure of cells *in vitro* to NMs is not routinely used to assess NM hazard. However, obtained data suggest that investigation of $[Ca^{2+}]_i$ could be a useful tool to screen NM toxicity in the future. Furthermore, electrophysiology has only been used to a very limit extent previously to investigate NM toxicity in excitable and non-excitable cells (e.g. Belyanskaya et al., 2009; Gavello et al., 2012; Leifert et al., 2013). Electrophysiology could therefore be used to a greater extent in future studies to investigate the toxicity exhibited by NMs especially as it directly addresses the patency of the lipid bilayer.

### 4.2. Cytokine production

This study demonstrated that Ag NMs elicited a dose and time dependent increase in MCP-1 and IL-8 production by differentiated HL-60 cells. Inhibitors of $Ca^{2+}$ signaling (BAPTA-AM, verapamil, SKF96365) and the antioxidant trolox reduced Ag NM mediated increases in cytokine production by differentiated HL-60 cells. This suggests that Ag NM mediated increases in $[Ca^{2+}]_i$ and ROS production may be involved in the production of pro-inflammatory cytokines by neutrophil-like cells. The ability of $Ca^{2+}$ and ROS production to control the production of inflammatory mediators following exposure to ufCB has been observed in macrophages (Brown et al., 2004a,b). In addition, this study observed an increase in $[Ca^{2+}]_i$ following Ag NM exposure, which is known to modulate cytokine production in neutrophils (Tintinger et al., 2005). Thus, we recommend that the influence of $Ca^{2+}$ and oxidant signaling on NM stimulated cytokine production continues to be investigated in cells in the future. It was unexpected that ufCB NMs did not induce a cytokine response, especially as our hypothesis was that changes in cytokine production were mediated by an increase in intracellular $Ca^{2+}$ and ufCB was able to stimulate a significant elevation in $[Ca^{2+}]_i$. However, this observation may be explained in a number of ways. Firstly, only a limited number of cytokines were investigated in this study and it is possible that ufCB stimulates the production of other cytokines that were not investigated (e.g. GROα). Secondly, a higher concentration of ufCB may have been required to stimulate a cytokine response in neutrophils. Lastly, it is known that ufCB (and other NMs) can interfere with cytokine analysis due to the adsorption of cytokines onto the NM surface which prevents their detection. Thus, it is possible that ufCB may stimulate an increase in cytokine production but these cytokines become bound to the ufCB surface, thus preventing their detection and measurement. We have previously demonstrated IL8 and TNFα adsorption onto ufCB (Brown et al., 2010).

### 4.3. Superoxide anion production

The release of ROS such as superoxide anions has been termed an oxidative/respiratory burst, and is essential to the elimination of foreign material and critical to the role of leukocytes in host defence (Goncalves et al., 2011). Superoxide anion production is mediated by NADPH oxidase, and the activation of NAPDH oxidase is a $Ca^{2+}$ dependent process (Bréchard and Tschirhart, 2008; Tintinger et al., 2005). Ag NMs were able to stimulate a dose dependent increase in superoxide anion production, which is likely to derive from their ability to stimulate an increase in $[Ca^{2+}]_i$. Further studies would be required to investigate the role of $[Ca^{2+}]_i$ in the respiratory burst stimulated by Ag NMs.

### 4.4. Cell viability

In terms of the impact of the NMs on cytotoxicity at 24 h, Ag and ZnO NMs were of relatively high toxicity, and ufCB, $TiO_2$ and MWCNT NMs were of relatively low toxicity. This ranking of toxicity of the same NM panel is comparable to that observed following the exposure of the C3A hepatocyte cell line (Kermanizadeh et al., 2013b), and the HK-2 renal epithelial cells (Kermanizadeh et al., 2013c) *in vitro*, as well as lung and liver tissue *in vivo* (Kermanizadeh et al., 2013a). All NMs have been extensively characterised previously (e.g. Stone et al., 1998; Singh et al., 2011; Klein et al., 2011; Kermanizadeh et al., 2013b). The physico-chemical characteristics of these NMs suggest that the toxicity of the ZnO NMs derives from their high solubility (40–50% soluble following a 24 h incubation in cell culture medium), and therefore release of $Zn^{2+}$ ions (Kermanizadeh et al., 2013b). Conversely, the solubility of the Ag NMs is low; <1% soluble following a 24 h incubation in cell culture medium (Kermanizadeh et al., 2013b) or in environmental aquatic test medium (Völker et al., 2013), and thus other physico-chemical properties (such as size and composition) are more likely to drive their toxicity. As the solubility of Ag NMs was known to be low in cell culture medium an ionic control was not included in this study. The effects on HL60 cells were typically observed at Ag NM concentrations of 4–8 μg/ml. At 4 μg/ml, 1% of the dose, i.e. approximately 40 ng/ml Ag ions could exist in solution in cell culture medium (Kermanizadeh et al., 2013b). However, due to the high chloride content of RPMI medium (several mg/ml), and a $K_{sp}$ (solubility product constant) for AgCl of $1.77 \times 10^{-10}$, only approximately 400 pg/ml $Ag^{+}$ ions are expected to exist in solution at this concentration. We therefore did not include $Ag^{+}$ ions in the exposure regime since such small quantities would be prone to preparation and measurement errors, and propose that if Ag ions should be responsible for the effects observed, this may be due to uptake of Ag NMs and subsequent ion release in the cell. Future studies are required to confirm this hypothesis. It is therefore likely that the effects observed are mediated by silver NMs and not ions released into the culture medium.

Ag NMs were able to induce $Ca^{2+}$ dependent apoptosis in cells in a dose dependent manner, 24 h post exposure. In contrast, ufCB and $TiO_2$ NMs did not stimulate apoptosis at the doses and time points investigated. It may be possible that ufCB and $TiO_2$ stimulate apoptosis via a $Ca^{2+}$ independent mechanism. As a result, light microscopy was also used to evaluate whether ufCB and $TiO_2$ NMs induced apoptosis in cells, and to confirm the impact of Ag NMs on cell viability. Visualisation of cells confirmed that Ag NMs induced cell death and that $TiO_2$ NMs and ufCB did not induce cell death at the concentrations tested (<125 μg/ml). Further evidence that $TiO_2$ and ufCB NMs did not induce cell death was confirmed from the findings of the alamar blue cytotoxicity assay performed in this study. NMs have also been demonstrated to induce cell death via etosis (e.g. Haase et al., 2014), and future studies could further investigate the role of this process in NM toxicity.

### 4.5. Hypothesis: mechanism of NM toxicity in neutrophils

Overall, our data support the hypothesis that some NMs can activate neutrophil-like cells via $Ca^{2+}$ and oxidant signaling (Fig. 11). It is hypothesised that NMs are able to stimulate a rise in intracellular $Ca^{2+}$ concentration in cells which is dictated by their physico-chemical characteristics and NM concentration

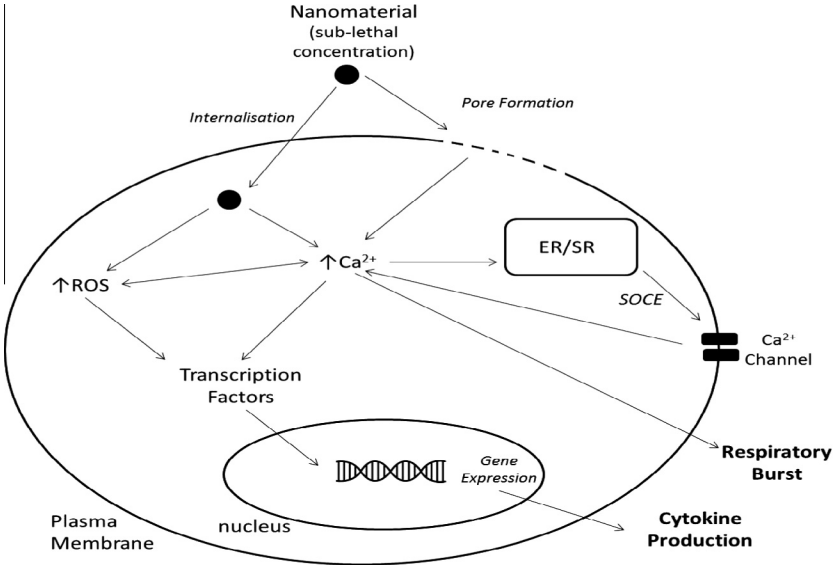


**Fig. 11.** Mode of action of NM toxicity in cells It is hypothesised that NMs stimulate an increase in $[Ca^{2+}]_i$ following exposure (at a sub-lethal concentration). Elevated $[Ca^{2+}]_i$ may be stimulated via NM mediated ROS production, store operated $Ca^{2+}$ entry (SOCE), or the formation of pores in the plasma membrane. The increase in $[Ca^{2+}]_i$ stimulates cytokine production and a respiratory burst. SR/ER = endoplasmic/sarcoplasmic reticulum.

administered. The increase in $[Ca^{2+}]_i$ could be dependent on NM mediated intracellular ROS production, and vice versa. A rise in $[Ca^{2+}]_i$ and intracellular ROS is likely to stimulate a respiratory burst and cause the activation of transcription factors (such as NF-κB) to promote the expression of pro-inflammatory cytokines. However, the applicability of this hypothesis to more diverse cell and NM types requires investigation.

## 5. Conclusion

Overall, the results from the study suggest that Ag NMs stimulate time and concentration dependent oxidative and inflammatory processes in neutrophil-like cells which are driven by changes in intracellular $Ca^{2+}$ and ROS concentration. In contrast, ufCB was less toxic, inducing increased intracellular $Ca^{2+}$ without induction of cytokine production or apoptosis. $TiO_2$ was ineffective with respect to induction of $Ca^{2+}$ changes as well as all other endpoints tested. This study therefore provided a more detailed understanding of the mechanism underlying the cellular response to NMs and how this can differ according to the physicochemical characteristics of NMs. The information obtained can be used to inform future studies which investigate the toxicological mechanism of action of NMs, guide NM toxicity testing by identifying more evidence based reliable and sensitive endpoints for hazard assessment and screening, and will help to generate a battery of tests that can indicate the potential consequences of NM exposure for human health. We suggest that evidence of the prominent role of $Ca^{2+}$ in the sub-lethal toxicity of NMs can be exploited in a novel approach to screen NM safety in the future. Future studies are required to determine if the findings are applicable to primary human neutrophils.

## Conflict of Interest

The authors declare that there are no conflicts of interest.

## Transparency Document

The Transparency document associated with this article can be found in the online version.

## Acknowledgements

The authors would like to thank Dr. Lesley Young, and Dr. David Mincher for kindly allowing us to use the fluorimeter located at Edinburgh Napier University.

## References

Abrikossova, N., Skoglund, C., Ahrén, M., Bengtsson, T., Uvdal, K., 2012. Effects of gadolinium oxide nanoparticles on the oxidative burst from human neutrophil granulocytes. Nanotechnology 23 (27), 275101.
Ahamed, M., Alhadlaq, H.A., Alam, J., Khan, M.A., Ali, D., Alarafi, S., 2013. Iron oxide nanoparticle-induced oxidative stress and genotoxicity in human skin epithelial and lung epithelial cell lines. Curr. Pharm. Des. 19 (37), 6681–6690.
Akhtar, M.J., Kumar, S., Alhadlaq, H.A., Alrokayan, S.A., Abu-Salah, K.M., Ahamed, M., 2013. Dose-dependent genotoxicity of copper oxide nanoparticles stimulated by reactive oxygen species in human lung epithelial cells. Toxicol. Ind. Health (Epub ahead of print).
Ali, D., Ahmed, M., Alarifi, S., Ali, H., 2014. Ecotoxicity of single-wall carbon nanotubes to freshwater snail *Lymnaea luteola* L.: Impacts on oxidative stress and genotoxicity. Environ. Toxicol. (Epub ahead of print)
Babin, K., Antoine, F., Goncalves, D.M., Girard, D., 2013. $TiO_2$, $CeO_2$ and ZnO nanoparticles and modulation of the degranulation process in human neutrophils. Toxicol. Lett. 221 (1), 57–63.
Baisch, B.L., Corson, N.M., Wade-Mercer, P., Gelein, R., Kennell, A.J., Oberdörster, G., Elder, A., 2014. Equivalent titanium dioxide nanoparticle deposition by intratracheal instillation and whole body inhalation: the effect of dose rate on acute respiratory tract inflammation. Part Fibre Toxicol. 11, 5.
Baktur, R.1, Patel, H., Kwon, S., 2011. Effect of exposure conditions on SWCNT-induced inflammatory response in human alveolar epithelial cells. Toxicol. In Vitro 25 (5), 1153–1160.
Belyanskaya, L., Weigel, S., Hirsch, C., Tobler, U., Krug, H.F., Wick, P., 2009. Effects of carbon nanotubes on primary neurons and glial cells. Neurotoxicology 30 (4), 702–711.
Bhattacharjee, S., Rietjens, I.M., Singh, M.P., Atkins, T.M., Purkait, T.K., Xu, Z., Regli, S., Shukaliak, A., Clark, R.J., Mitchell, B.S., Alink, G.M., Marcelis, A.T., Fink, M.J., Veinot, J.G., Kauzlarich, S.M., Zuilhof, H., 2013. Cytotoxicity of surface-functionalized silicon and germanium nanoparticles: the dominant role of surface charges. Nanoscale 5 (11), 4870–4883.
Bréchard, S., Tschirhart, E.J., 2008. Regulation of superoxide production in neutrophils: role of $Ca^{2+}$ influx. J. Leukoc Biol. 84 (5), 1223–1237.
Brown, G.M., Brown, D.M., Slight, J., Donaldson, K., 1991. Persistent biological reactivity of quartz in the lung: raised protease burden compared with a non-pathogenicmineral dust and microbial particles. Br. J. Ind. Med. 48 (1), 61–69.
Brown, D.M., Stone, V., Findlay, P., MacNee, W., Donaldson, K., 2000. Increased inflammation and intracellular $Ca^{2+}$ caused by ultrafine carbon black is independent of transition metals or other soluble components. Occup. Environ. Med. 57 (10), 685–691.
Brown, D.M., Wilson, M.R., MacNee, W., Stone, V., Donaldson, K., 2001. Size-dependent pro-inflammatory effects of ultrafine polystyrene particles: a role for

surface area and oxidative stress in the enhanced activity of ultrafines. Toxicol. Appl. Pharmacol. 175, 191–199.
Brown, D.M., Donaldson, K., Borm, P.J., Schins, R.P., Dehnhardt, M., Gilmour, P., Jimenez, L.A., Stone, V., 2004a. $Ca^{2+}$ and ROS-mediated activation of transcription factors and TNF-cytokine gene expression in macrophages exposed to ultrafine particles. Am. J. Physiol.: Lung Cell. Mol. Physiol. 286, L344–L353.
Brown, D., Donaldson, K., Stone, V., 2004b. Effects of PM10 in human peripheral blood monocytes and J774 macrophages. Respir. Res. 5 (1), 29.
Brown, D.M., Dickson, C., Duncan, P., Al-Attili, F., Stone, V., 2010. Interaction between nanoparticles and cytokine proteins: impact on protein and particle functionality. Nanotechnology 21, 215104.
Couto, D., Freitas, M., Vilas-Boas, V., Dias, I., Porto, G., Lopez-Quintela, M.A., Rivas, J., Freitas, P., Carvalho, F., Fernandes E., 2014. Interaction of polyacrylic acid coated and non-coated iron oxide nanoparticles with human neutrophils. Toxicol. Lett. 10, 225(1), 57–65.
Donaldson, K., Bolton, R.E., Jones, A., Brown, G.M., Robertson, M.D., Slight, J., Cowie, H., Davis, J.M., 1988. Kinetics of the bronchoalveolar leucocyte response in rats during exposure to equal airborne massconcentrations of quartz, chrysotile asbestos, or titanium dioxide. Thorax 43 (7), 525–533.
Donaldson, K., Stone, V., Clouter, A., Renwick, L., MacNee, W., 2001. Ultrafine particles. Occup. Environ. Med. 2001 (58), 211–216.
Donaldson, K., Stone, V., Borm, P.J., Jimenez, L.A., Gilmour, P.S., Schins, R.P., Knaapen, A.M., Rahman, I., Faux, S.P., Brown, D.M., MacNee, W., 2003. Oxidative stress and $Ca^{2+}$ signaling in the adverse effects of environmental particles (PM10). Free Radic. Biol. Med. 1, 34(11), 1369–1382.
Duffin, R., Tran, L., Brown, D., Stone, V., Donaldson, K., 2007. Proinflammogenic effects of low-toxicity and metal nanoparticles in vivo and in vitro: highlighting the role of particle surface area and surface reactivity. Inhal Toxicol. 19 (10), 849–856.
Ermak, G., Davies, K.J., 2002. $Ca^{2+}$ and oxidative stress: from cell signaling to cell death. Mol. Immunol. 38 (10), 713–721.
European Commission, 2011. Recommendation on the definition of a nanomaterial. <http://ec.europa.eu/environment/chemicals/nanotech/pdf/commission_recommendation.pdf>.
Farrera, C., Bhattacharya, K., Lazzaretto, B., Andón, F.T., Hultenby, K., Kotchey, G.P., Star, A., Fadeel, B., 2014. Extracellular entrapment and degradation of single-walled carbon nanotubes. Nanoscale 19 (Epub ahead of print).
Ferin, J., Oberdorster, G., Penney, D.P., 1992. Pulmonary retention of ultrafine and fine particles in rats. Am. J. Respir.: Cell. Mol. Biol. 6, 535–542.
Gaiser, B.K., Hirn, S., Kermanizadeh, A., Kanase, N., Fytianos, K., Wenk, A., Haberl, N., Brunelli, A., Kreyling, W.G., Stone, V., 2013. Effects of silver nanoparticles on the liver and hepatocytes in vitro. Toxicol. Sci. 131 (2), 537–547.
Gavello, D., Vandael, D.H., Cesa, R., Premoselli, F., Marcantoni, A., Cesano, F., Scarano, D., Fubini, B., Carbone, E., Fenoglio, I., Carabelli, V., 2012. Altered excitability of cultured chromaffin cells following exposure to multi-walled carbon nanotubes. Nanotoxicology 6 (1), 47–60.
Gerloff, K., Albrecht, C., Boots, A.W., Förster, I., Schins, R.P., 2011. Particles which may occur in food or food packaging can exert cytotoxicity and (oxidative) DNA damage in target cells of the human intestine. Nanotoxicology 5 (2), 282–283.
Gerloff, K., Pereira, D.I., Faria, N., Boots, A.W., Kolling, J., Förster, I., Albrecht, C., Powell, J.J., Schins, R.P., 2013. Influence of simulated gastrointestinal conditions on particle-induced cytotoxicity and interleukin-8 regulation in differentiated and undifferentiated Caco-2 cells. Nanotoxicology 7 (4), 353–366.
Gomes, T., Pereira, C.G., Cardoso, C., Sousa, V.S., Teixeira, M.R., Pinheiro, J.P., Bebianno, M.J., 2014. Effects of silver nanoparticles exposure in the mussel *Mytilus galloprovincialis*. Mar. Environ. Res. 101, 208–214.
Gonçalves, D.M., Chiasson, S., Girard, D., 2010. Activation of human neutrophils by titanium dioxide ($TiO_2$) nanoparticles. Toxicol. In Vitro 24 (3), 1002–1008.
Goncalves, D.M., de Liz, R., Girard, D., 2011. Activation of neutrophils by nanoparticles. Sci. World J. 11, 1877–1885.
Haase, H., Fahmi, A., Mahltig, B., 2014. Impact of silver nanoparticles and silver ions on innate immune cells. J. Biomed. Nanotechnol. 10 (6), 1146–1156.
Huang, C.C., Aronstam, R.S., Chen, D.R., Huang, Y.W., 2010. Oxidative stress, $Ca^{2+}$ homeostasis, and altered gene expression in human lung epithelial cells exposed to ZnO nanoparticles. Toxicol. In Vitro 24 (1), 45–55.
Jacobsen, N.R., Møller, P., Jensen, K.A., Vogel, U., Ladefoged, O., Loft, S., Wallin, 2009. Lung inflammation and genotoxicity following pulmonary exposure to nanoparticles in ApoE-/- mice. Part Fibre Toxicol. 12 (6), 2.
Jacobsen, N.R., Pojano, G., Wallin, H., Jensen, K.A., 2010. Nanomaterial dispersion protocol for toxicological studies in ENPRA. Internal ENPRA Project Report. The National Research Centre for the Working Environment.
Jiménez, L.A., Drost, E.M., Gilmour, P.S., Rahman, I., Antonicelli, F., Ritchie, H., MacNee, W., Donaldson, K., 2002. PM(10)-exposed macrophages stimulate a proinflammatory response in lung epithelial cells via TNF-alpha. Am. J. Physiol. Lung Cell. Mol. Physiol. 282 (2), L237–L248.
Jovanović, B., Anastasova, L., Rowe, E.W., Zhang, Y., Clapp, A.R., Palić, D., 2011. Effects of nanosized titanium dioxide on innate immune system of fathead minnow (*Pimephales promelas* Rafinesque, 1820). Ecotoxicol. Environ. Saf. 74 (4), 675–683.
Kermanizadeh, A., Brown, D.M., Hutchison, G.R., Stone, V., 2013a. Engineered nanomaterial impact in the liver following exposure via an intravenous route – the role of polymorphonuclear leukocytes and gene expression in the organ. J. Nanomed. Nanotechol. 4, 157.
Kermanizadeh, A., Pojana, G., Gaiser, B.K., Birkedal, R., Bilanicová, D., Wallin, H., Jensen, K.A., Sellergren, B., Hutchison, G.R., Marcomini, A., Stone, V., 2013b. In vitro assessment of engineered nanomaterials using a hepatocyte cell line: cytotoxicity, pro-inflammatory cytokines and functional markers. Nanotoxicology 7 (3), 301–313.
Kermanizadeh, A., Vranic, S., Boland, S., Moreau, K., Baeza-Squiban, A., Gaiser, B.K., Andrzejczuk, L.A., Stone, V., 2013c. An in vitro assessment of panel of engineered nanomaterials using a human renal cell line: cytotoxicity, pro-inflammatory response, oxidative stress and genotoxicity. BMC Nephrol. 14, 96.
Kim, H.R., Kim, M.J., Lee, S.Y., Oh, S.M., Chung, K.H., 2011. Genotoxic effects of silver nanoparticles stimulated by oxidative stress in human normal bronchial epithelial (BEAS-2B) cells. Mutat. Res. 24, 726(2), 129–35.
Klein, C.L., Comero, S., Stahlmecke, B., Romazanov, J., Kuhlbusch, T.A.J., Van Doren, E., De Temmerman, P-J. Mast J., Wick, P., Krug, H., Locoro, G., Hund-Rinke, K., Kördel, W., Friedrichs, S., Maier, G., Werner, J., Linsinger, T., Gawlik, B.M., 2011. NM-Series of Representative Manufactured Nanomaterials, NM-300 Silver Characterisation, Stability, Homogeneity. JRC Scientific and Technical Reports. <http://bookshop.europa.eu/en/nm-series-of-representative-manufactured-nanomaterials-pbLBNA24693/downloads/LB-NA-24693-EN-C/LBNA24693ENC_002.pdf?FileName=LBNA24693ENC_002.pdf&SKU=LBNA24693ENC_PDF&CatalogueNumber=LB-NA-24693-EN-C>.
Krause, K.H., Welsh, M.J., 1990. Voltage-dependent and Ca2(+)-activated ion channels in human neutrophils. J. Clin. Invest. 85 (2), 491–498.
Leifert, A., Pan, Y., Kinkeldey, A., Schiefer, F., Setzler, J., Scheel, O., Lichtenbeld, H., Schmid, G., Wenzel, W., Jahnen-Dechent, W., Simon, U., 2013. Differential hERG ion channel activity of ultrasmall gold nanoparticles. Proc. Natl. Acad. Sci. USA 110 (20), 8004–8009. http://dx.doi.org/10.1073/pnas.1220143110 (Epub 2013 April 29).
Li, N., Venkatesan, M.I., Miguel, A., Kaplan, R., Gujuluva, C., Alam, J., Nel, A., 2000. Induction of heme oxygenase-1 expression in macrophages by diesel exhaust particle chemicals and quinones via the antioxidant-responsive element. J. Immunol. 165 (6), 3393–3401.
Li, N., Kim, S., Wang, M., Froines, J., Sioutas, C., Nel, A., 2002. Use of a stratified oxidative stress model to study the biological effects of ambient concentrated and diesel exhaust particulate matter. Inhal. Toxicol. 14 (5), 459–486.
Li, N., Hao, M., Phalen, R.F., Hinds, W.C., Nel, A.E., 2003. Particulate air pollutants and asthma. A paradigm for the role of oxidative stress in PM-induced adverse health effects. Clin. Immunol. 109 (3), 250–265.
Li, N., Xia, T., Nel, A.E., 2008. The role of oxidative stress in ambient particulate matter-induced lung diseases and its implications in the toxicity of engineered nanoparticles. Free Radic. Biol. Med. 44 (9), 1689–1699.
Luo, M., Deng, X., Shen, X., Dong, L., Liu, Y., 2012. Comparison of cytotoxicity of pristine and covalently functionalized multi-walled carbon nanotubes in RAW 264.7 macrophages. J. Nanosci. Nanotechnol. 12 (1), 274–283.
McCarthy, J., Inkielewicz-Stępniak, I., Corbalan, J.J., Radomski, M.W., 2012. Mechanisms of toxicity of amorphous silica nanoparticles on human lung submucosal cells in vitro: protective effects of fisetin. Chem. Res. Toxicol. 2, 25(10), 2227–2235.
Möller, W., Brown, D.M., Kreyling, W.G., Stone, V., 2005. Ultrafine particles cause cytoskeletal dysfunctions in macrophages: role of intracellular $Ca^{2+}$. Part Fibre Toxicol. 4 (2), 7.
Monteiller, C., Tran, L., MacNee, W., Faux, S., Jones, A., Miller, B., Donaldson, K., 2007. The pro-inflammatory effects of low-toxicity low-solubility particles, nanoparticles and fine particles, on epithelial cells in vitro: the role of surface area. Occup. Environ. Med. 64 (9), 609–615.
Monteiro-Riviere, N.A., Nemanich, R.J., Inman, A.O., Wang, Y.Y., Riviere, J.E., 2005. Multi-walled carbon nanotube interactions with human epidermal keratinocytes. Toxicol. Lett. 15, 155(3), 377–84.
Murphy, F.A., Poland, C.A., Duffin, R., Al-Jamal, K.T., Ali-Boucetta, H., Nunes, A., Byrne, F., Prina-Mello, A., Volkov, Y., Li, S., Mather, S.J., Bianco, A., Prato, M., Macnee, W., Wallace, W.A., Kostarelos, K., Donaldson, K., 2011. Length-dependent retention of carbon nanotubes in the pleural space of mice initiates sustained inflammation and progressive fibrosis on the parietal pleura. Am. J. Pathol. 178 (6), 2587–2600.
Nel, A., Xia, T., Mädler, L., Li, N., 2006. Toxic potential of materials at the nanolevel. Science 3, 311(5761), 622–7.
Oberdörster, G., Ferin, J., Morrow, P.E., 1992. Volumetric loading of alveolar macrophages (AM): a possible basis for diminished AM-mediated particleclearance. Exp. Lung Res. 18 (1), 87–104.
O'Flaherty, J.T., Rossi, A.G., Jacobson, D.P., Redman, J.F., 1991. Roles of $Ca^{2+}$ in human neutrophil responses to receptor agonists. Biochem. J. 277, 705–711.
Park, J., Lim, D.H., Lim, H.J., Kwon, T., Choi, J.S., Jeong, S., Choi, I.H., Cheon, J., 2011. Size dependent macrophage responses and toxicological effects of Ag nanoparticles. Chem. Commun. (Camb) 47 (15), 4382–4384.
Peters, A., Wichmann, H.E., Tuch, T., Heinrich, J., Heyder, J., 1997. Respiratory effects are associated with the number of ultrafine particles. Am. J. Respir. Crit. Care Med. 155, 1376–1383.
Poland, C.A., Duffin, R., Kinloch, I., Maynard, A., Wallace, W.A., Seaton, A., Stone, V., Brown, S., MacNee, W., Donaldson, K., 2008. Carbon nanotubes introduced into the abdominal cavity of mice show asbestos-like pathogenicity in a pilot study. Nat. Nanotechnol. 3, 423–428.
Pope, C.A., Dockery, D.W., 1999. Epidemiology of particle effects. In: Holgate, S.T., Samet, J.M., Koren, H.S. (Eds.), Air Pollution and Health. Academic Press, San Diego, pp. 673–705.
Risom, L., Møller, P., Loft, S., 2005. Oxidative stress-induced DNA damage by particulate air pollution. Mutat Res. 592 (1–2), 119–137.

Samberg, M.E., Oldenburg, S.J., Monteiro-Riviere, N.A., 2010. Evaluation of silver nanoparticle toxicity in skin in vivo and keratinocytes in vitro. Environ. Health Perspect. 118 (3), 407–413.

Sayes, C.M., Reed, K.L., Warheit, D.B., 2007. Assessing toxicity of fine and nanoparticles: comparing in vitro measurements to in vivo pulmonary toxicity profiles. Toxicol. Sci. 97 (1), 163–180 (Epub 2007 February 14).

Schaeublin, N.M., Braydich-Stolle, L.K., Schrand, A.M., Miller, J.M., Hutchison, J., Schlager, J.J., Hussain, S.M., 2011. Surface charge of gold nanoparticles mediates mechanism of toxicity. Nanoscale 3, 410–420.

Schmid, O., Möller, W., Semmler-Behnke, M., Ferron, G.A., Karg, E., Lipka, J., Schulz, H., Kreyling, W.G., Stoeger, T., 2009. Dosimetry and toxicology of inhaled ultrafine particles. Biomarkers 14 (Suppl 1), 67–73.

Seaton, A., MacNee, W., Donaldson, K., Godden, D., 1995. Particulate air pollution and acute health effects. Lancet 345, 176–178.

Sharma, V., Anderson, D., Dhawan, A., 2011. Zinc oxide nanoparticles induce oxidative stress and genotoxicity in human liver cells (HepG2). J. Biomed. Nanotechnol. 7 (1), 98–99.

Shukla, A., Timblin, C., BeruBe, K., Gordon, T., McKinney, W., Driscoll, K., Vacek, P., Mossman, B.T., 2000. Inhaled particulate matter causes expression of nuclear factor (NF)-kappaB-related genes and oxidant-dependent NF-kappaB activation in vitro. Am. J. Respir. Cell. Mol. Biol. 23 (2), 182–187.

Shukla, R.K., Sharma, V., Pandey, A.K., Singh, S., Sultana, S., Dhawan, A., 2011. ROS-mediated genotoxicity induced by titanium dioxide nanoparticles in human epidermal cells. Toxicol. In Vitro 25 (1), 231–241.

Shvedova, A.A., Kisin, E.R., Murray, A.R., Gorelik, O., Arepalli, S., Castranova, V., Young, S.H., Gao, F., Tyurina, Y.Y., Oury, T.D., Kagan, V.E., 2007. Vitamin E deficiency enhances pulmonary inflammatory response and oxidative stress induced by single-walled carbon nanotubes in C57BL/6 mice. Toxicol. Appl. Pharmacol. 221 (3), 339–348.

Singh, C., Friedrichs, S., Levin, M., Birkedal, R., Jensen, K.A., Pojana, G., Wohlleben, W., Schulte, S., Wiench, K., Turney, T., Koulaeva, O., Marshall, D., Hund-Rinke, K., Kördel, W., Van Doren, E., De Temmerman, P-J, Abi Daoud Francisco, M., Mast, J., Gibson, N., Koeber, R., Linsinger, T., Klein, C.L., 2011. NM-Series of Representative Manufactured Nanomaterials. Zinc Oxide NM-110, NM-111, NM-112, NM-113 Characterisation and Test Item Preparation. <http://publications.jrc.ec.europa.eu/repository/bitstream/111111111/23031/1/lana25066enn.pdf>.

Stone, V., Shaw, J., Brown, D.M., MacNee, W., Faux, S.P., Donaldson, K., 1998. The role of oxidative stress in the prolonged inhibitory effect of ultrafine carbon black on epithelial cell function. Toxicol. In Vitro 12, 649–659.

Stone, V., Tuinman, M., Vamvakopoulos, J.E., Shaw, J., Brown, D., Petterson, S., Faux, S.P., Borm, P., MacNee, W., Michaelangeli, F., Donaldson, K., 2000. Increased $Ca^{2+}$ influx in a monocytic cell line on exposure to ultrafine carbon black. Eur. Respir. J. 15 (2), 297–303.

Stone, V., Johnston, H., Clift, M.J., 2007. Air pollution, ultrafine and nanoparticle toxicology: cellular and molecular interactions. IEEE Trans. Nanobiosci. 6 (4), 331–340.

Stone, V., Pozzi-Mucelli, S., Tran, L., Aschberger, K., Sabella, S., Vogel, U., Poland, C., Balharry, D., Fernandes, T., Gottardo, S., Hankin, S., Hartl, M.G., Hartmann, N., Hristozov, D., Hund-Rinke, K., Johnston, H., Marcomini, A., Panzer, O., Roncato, D., Saber, A.T., Wallin, H., Scott-Fordsmand, J.J., 2014. ITS-NANO-prioritising nanosafety research to develop a stakeholder driven intelligent testing strategy. Part Fibre Toxicol. 13 (11), 9.

Suliman, Y.A.O., Ali, D., Alarifi, S., Harrath, A.H., Mansour, L., Alwasel, S.H., 2013. Evaluation of cytotoxic, oxidative stress, proinflammatory and genotoxic effect of silver nanoparticles in human lung epithelial cells. Environ. Toxicol. (Epub ahead of print)

Takahashi, A., Camacho, P., Lechleiter, J.D., Herman, B., 1999. Measurement of intracellular $Ca^{2+}$. Physiol. Rev. 79 (4), 1089–1125.

Tarantini, A., Lanceleur, R., Mourot, A., Lavault, M.T., Casterou, G., Jarry, G., Hogeveen, K., Fessard, V., 2014. Toxicity, genotoxicity and proinflammatory effects of amorphous nanosilica in the human intestinal Caco-2 cell line. Toxicol. In Vitro (Epub ahead of print).

Tintinger, G., Steel, H.C., Anderson, R., 2005. Taming the neutrophil: $Ca^{2+}$ clearance and influx mechanisms as novel targets for pharmacological control. Clin. Exp. Immunol. 141 (2), 191–200.

Trump, B.F., Berezesky, I.K., 1995. $Ca^{2+}$-mediated cell injury and cell death. FASEB J. 9 (2), 219–228.

Völker, C., Boedicker, C., Daubenthaler, J., Oetken, M., Oehlmann, J., 2013. Comparative toxicity assessment of nanosilver on three Daphnia species in acute, chronic and multi-generation experiments.PLoS One 7, 8(10), e75026.

Wilson, M.R., Lightbody, J.H., Donaldson, K., Sales, J., Stone, V., 2002. Interactions between ultrafine particles and transition metals in vivo and in vitro. Toxicol. Appl. Pharmacol. 184 (3), 172–179.

Xia, T., Kovochich, M., Brant, J., Hotze, M., Sempf, J., Oberley, T., Sioutas, C., Yeh, J.I., Wiesner, M.R., Nel, A.E., 2006. Comparison of the abilities of ambient and manufactured nanoparticles to induce cellular toxicity according to an oxidative stress paradigm. Nano Lett. 6 (8), 1794–1807.

Xiao, G.G., Wang, M., Li, N., Loo, J.A., Nel, A.E., 2003. Use of proteomics to demonstrate a hierarchical oxidative stress response to diesel exhaust particle chemicals in a macrophage cell line. J. Biol. Chem. 278 (50), 50781–50790.